PTEN regulates motility but not directionality during leukocyte chemotaxis

Rosa Ana Lacalle, Concepción Gómez-Moutón, Domingo F. Barber, Sonia Jiménez-Baranda, Emilia Mira, Carlos Martínez-A., Ana C. Carrera and Santos Mañes*

Department of Immunology and Oncology, Centro Nacional de Biotecnología/CSIC, UAM Campus de Cantoblanco, 28049 Madrid, Spain
*Author for correspondence (e-mail: smanes@cnb.uam.es)

Accepted 16 September 2004
Journal of Cell Science 117, 6207-6215 Published by The Company of Biologists 2004
doi:10.1242/jcs.01545

Summary

The localization at opposite cell poles of phosphatidylinositol-3 kinases and PTEN (phosphatase and tensin homolog on chromosome 10) governs *Dictyostelium* chemotaxis. To study this model in mammalian cells, we analyzed the dynamic redistribution of green fluorescent protein (GFP)-tagged PTEN chimeras during chemotaxis. N- or C-terminus GFP-tagged PTEN was distributed homogenously in the cytoplasm of chemotaxing PTEN-negative Jurkat cells and PTEN-positive HL60 cells. Moreover, we did not detect uropod accumulation of endogenous PTEN in chemoattractant-stimulated HL60 cells. Cell fractionation indicated that both endogenous and ectopically expressed PTEN were confined largely to the cytosol, and that chemoattractant stimulation did not alter this location. PTEN re-expression in Jurkat cells or PTEN depletion by specific siRNA in HL60 cells did not affect cell gradient sensing; PTEN nonetheless modulated chemoattractant-induced actin polymerization and the speed of cell movement. The results suggest a role for PTEN in regulating actin polymerization, but not directionality during mammalian cell chemotaxis.

Supplementary material available online at
http://jcs.biologists.org/cgi/content/full/117/25/6207/DC1

Key words: Polarization, Lipid rafts, Cell migration, PI3K, Actin cytoskeleton

Introduction

Chemotaxis is a fundamental response by which a cell senses the direction of external stimulus and responds by polarizing and migrating toward the source. Activation of seven-transmembrane receptors coupled to heterotrimeric G proteins (GPCR) is the first step in this sensing process in response to a wide variety of external signals, including non-GPCR agonists (Mira et al., 2001). Generation of phosphatidylinositol (3,4,5)-trisphosphate PtdIns(3,4,5)P_3 at the cell front is an early event in *Dictyostelium* and leukocyte chemotaxis; PtdIns(3,4,5)P_3 is considered the initial local activator used by the cell to sense and orient in chemoattractant gradients (Funamoto et al., 2002; Iijima and Devreotes, 2002; Li et al., 2003; Xu et al., 2003). In *Dictyostelium,* PtdIns(3,4,5)P_3 is restricted to the leading edge due to the location at the cell front of phosphoinositide-3 kinases (PI3Ks) [the enzymes that produce PtdIns(3,4,5)P_3] and PTEN [the enzyme that dephosphorylates the 3′ position of this lipid, at the cell sides and rear (Funamoto et al., 2002; Iijima and Devreotes, 2002)]. Whether this model can be extended to mammalian cells is debatable; whereas PI3K translocates from the cytosol to the leading edge in chemotaxing leukocytes (Gómez-Moutón et al., 2004), the precise location of PTEN in these cells is disputed (Li et al., 2003; Xu et al., 2003).

PTEN is a multifunctional enzyme with dual protein and lipid phosphatase activities (Seminario and Wange, 2002). The physiological lipid substrate of PTEN is PtdIns(3,4,5)P_3 and, to a lesser extent, PtdIns(3,4)P_2; PTEN thus antagonizes PI3K activity (Maehama and Dixon, 1998). Several protein substrates of PTEN have also been proposed, including focal adhesion kinase (FAK) and PTEN itself (Gu et al., 1999; Raftopoulou et al., 2004). In addition to its ability to suppress cell growth and survival (Borlado et al., 2000; Stambolic et al., 1998), evidence suggests that PTEN controls mammalian cell movement. *Pten*$^{-/-}$ fibroblasts show an increased migration rate, which is reduced after expression of wild-type PTEN in these cells (Liliental et al., 2000; Tamura et al., 1998). Although this phenotype is common to cells that have lost PTEN expression, there are also apparently contradictory findings. Some studies suggest that loss of PTEN increases B-cell chemotaxis to CXCL12 (Fox et al., 2002; Suzuki et al., 2003), whereas another group reported reduced chemotaxis in *pten*$^{-/-}$ B cells (Anzelon et al., 2003).

The mechanism by which PTEN regulates cell migration is unclear. In some cases, the increased cell migration has been attributed to augmented PtdIns(3,4,5)P_3 levels (Liliental et al., 2000; Tamura et al., 1998). Nonetheless, the PTEN effect on migration was also ascribed to its protein phosphatase activity. Indeed, expression of the naturally occurring PTEN mutant G129E, which has lost lipid phosphatase activity but retains protein phosphatase activity, inhibited migration of some tumor cells (Tamura et al., 1999); this effect might be mediated by PTEN-induced dephosphorylation of FAK. More recent evidence suggests a role for PTEN C2 domain phosphorylation in the inhibition of PTEN-deficient human glioma cell migration, independent of its lipid phosphatase activity

(Raftopoulou et al., 2004). The mechanism by which PTEN affects cell migration may be closely linked to its location in moving cells. For example, it is difficult to reconcile the model of FAK dephosphorylation by PTEN with the location of PTEN at the cell rear, as FAK is enriched at the leading edge of fibroblast and lymphocytes (Friedl et al., 1998).

Here we analyzed the dynamic redistribution of GFP-tagged PTEN chimeras in chemotaxing cells. In PTEN-deficient Jurkat T cells (Xu et al., 2002) and in HL60 cells (which express endogenous PTEN), both N- and C-terminal GFP-tagged PTEN (GFP-PTEN or PTEN-GFP, respectively) showed cytoplasmic distribution almost identical to that of ds-Red2 fluorescent protein (RFP) cotransfected into these cells. The cytosolic restriction of PTEN, confirmed by cell fractionation, was independent of its catalytic activity. PTEN re-expression in Jurkat cells or PTEN depletion with specific siRNA in HL60 cells did not affect chemotaxis toward specific attractants. By contrast, catalytically active PTEN diminished chemoattractant-induced actin polymerization, and diminished cell speed. Whereas these findings indicate a role for PTEN in leukocyte motility, the data suggest that some chemoattractant signal amplification mechanisms are not conserved between *Dictyostelium* and mammalian cells.

Materials and Methods

Cloning and expression constructs

cDNA encoding human PTEN was a gift of R. Pulido (CIC, Valencia, Spain) and the PTEN-C/S (C124S) mutants, generated with the Quick Change site-directed mutagenesis kit (Stratagene) were subcloned in pEGFP-N3 and pEGFP-C2 vectors (Clontech) to generate the GFP-chimeras. PTEN and PTEN-C/S cDNA were subcloned in the bicistronic plasmid pRV-GFP (Genetrix, Spain). pRFP-GPI was obtained as described (Gómez-Moutón et al., 2004). Jurkat and HL60 cells differentiated in dimethyl sulfoxide (2×10^7 cells) were transfected by electroporation (BioRad) or by using the T-cell Nucleofector Kit (Amaxa Biosystem) with GFP-PTEN, PTEN-GFP or PTEN-C/S-GFP (C124S), or with PTEN or PTEN-C/S cDNA subcloned in the bicistronic plasmid pRV-GFP. Expression was analyzed 6-14 hours post-transfection by FACS (Coulter) and live cells were isolated on Ficoll gradients. In vitro PTEN phosphatase activity was measured in extracts of Jurkat cells transfected with the different chimeras or untagged PTEN in a Malachite-Green-based assay (Upstate Biochemicals, #17-351), using PtdIns(3,4,5)P_3 (Echelon) as a substrate, according to the manufacturer's instructions. An affinity purified, constitutive active PTEN form supplied with the kit was used as positive control.

siRNA experiments

HL60 cells were transfected with a pool of PTEN-specific siRNA or with pooled non-specific siRNA duplexes (100 nM; SMARTpool, Dharmacon) using Jet-PEI (Polyplus transfection). Control and PTEN-specific siRNA were co-transfected with a Cy3-labeled non-specific duplex control (Dharmacon), which were used to determine transfection efficiency (98-100%) by FACS. Silencing was confirmed 24-48 hours post-transfection by western blot.

Time-lapse confocal videomicroscopy and chemotaxis assays

Real-time cell chemotaxis was studied by time-lapse confocal microscopy, as described (Gómez-Moutón et al., 2004). Starved cells were plated (1 hour, 37°C) on fibronectin (Fn)-coated chamber coverslips (Nunc). Chemotaxis studies were performed at 37°C using a heating plate and a micromanipulation system (Narishige) adapted to a Leica confocal microscope. Stimulus was supplied in micropipettes (1-2 μm) prepared in a Kopf pipette puller using thin-wall glass capillaries with an inner filament (Clark Electromedical Instruments), filled with CXCL12 (100 nM; Peprotech) or *f*MLP (100 nM; Sigma) in serum-free RPMI and sealed at the back. Fluorescence and phase contrast images were recorded at established time intervals and videos were processed with NIH-Image J software. Fluorescence scanning was performed with MicroImage software (Olympus Optical). Cell motility speed and movement paths were analyzed with MetaMorph Imaging System (Universal Imaging).

For transwell assays, $1\text{-}2\times10^5$ PTEN-expressing Jurkat cells, or Jurkat cells pretreated with LY294002 or siRNA-transfected HL60 cells in serum-free medium were seeded in the upper chamber; lower chambers were filled with serum-free medium alone or containing CXCL12 (25 nM) or *f*MLP (100 nM). After incubation (2.5 hours, 37°C), cell number in the lower chamber was estimated by FACS. The percentage of migrating cells was calculated as the quotient between the number of migrating fluorescent cells in the lower chamber and the fluorescent cells in the initial input (×100).

Immunofluorescence

HL60 or CEM cells were plated on Fn-coated slides 12 hours before assay, starved, and stimulated (10 minutes, 37°C) with 100 nM *f*MLP (HL60 cells), then washed and fixed with 3.7% paraformaldehyde (15 minutes, 20°C) in PBS. Cells were then permeabilized with 0.1% Triton X-100 (5 minutes, 20°C) and incubated (1 hour, 4°C) with a PTEN antibody (Transduction Laboratories), followed by Cy3-conjugated second antibody (Jackson ImmunoResearch). Samples were mounted in Vectashield medium and images recorded in a confocal microscope (Leica).

Cell subfractionation and western blot

A crude membrane fraction was obtained by cell passage through a 30-gauge needle in 50 mM Tris-HCl pH 7.5, plus a protease and phosphatase inhibitor cocktail. Cleared supernatant was centrifuged (166,000 ***g***, 1 hour, 4°C) to precipitate the membrane fraction. Supernatant was collected and the precipitate resuspended in 50 mM Tris-HCl, pH 7.5, 1% Triton X-100, plus protease and phosphatase inhibitors. Normalized protein amounts (micro BCA, Pierce) for each fraction were resolved in SDS-PAGE and analyzed by sequential blotting with anti-transferrin receptor (Zymed), anti-p85 PI3K (Upstate Biotech), anti-tubulin (Sigma) and anti-PTEN (Santa Cruz Biotech) antibodies. To determine phospho-AKT index, serum-depleted cells were lysed with RIPA (50 mM Tris-HCl, pH 7.5, 0.15 M NaCl, 0.1% SDS, 0.5% deoxycholate, 1% NP40) and equal protein amounts blotted sequentially with anti-phospho-AKT (Transduction Laboratories), anti-AKT (Upstate Biotech) and anti-PTEN antibodies. Densitometry was performed with NIH Image software.

F-actin polymerization assay

Starved cells were stimulated with CXCL12 (100 nM, 37°C), fixed in 3.7% paraformaldehyde (10 minutes, 20°C) and resuspended sequentially in Cytofix (10 minutes, 4°C) and Permwash solution (Pharmingen). F-actin was stained using Alexa fluor 633 phalloidin (Molecular Probes; 2 U/ml, 20 minutes, 4°C) in Permwash. Cells were then washed and analyzed in a Cytomics FC-500 cytometer (Beckman-Coulter).

Results

Characterization of PTEN chimeras

To analyze PTEN dynamics in living cells, we constructed

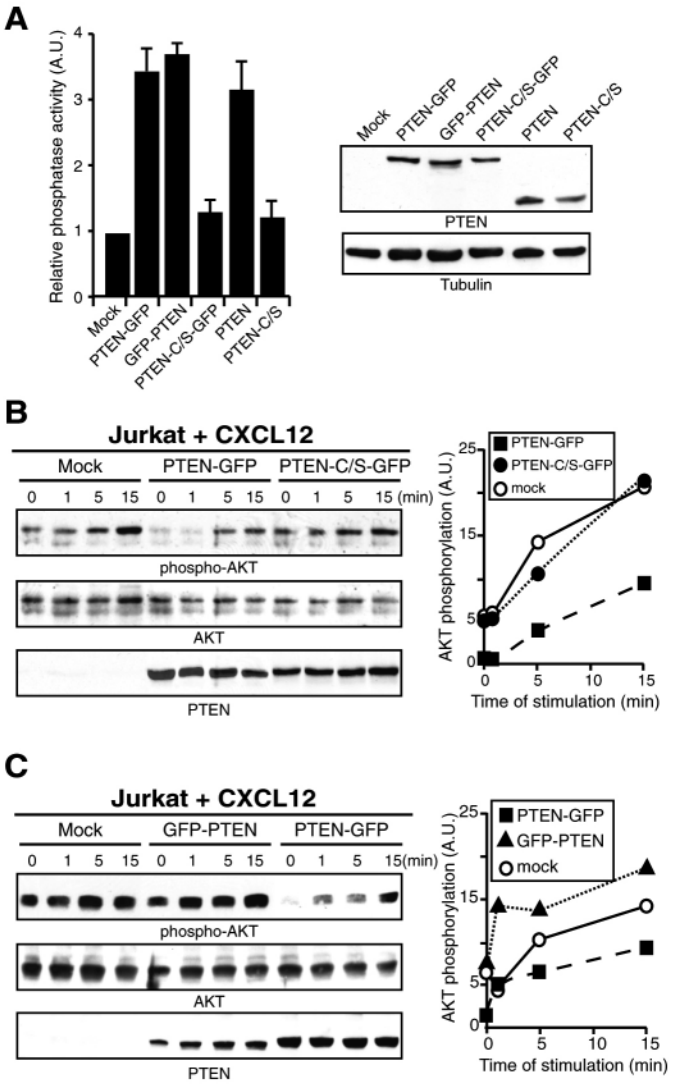

Fig. 1. Biochemical characterization of PTEN chimeras. (A) Extracts from Jurkat cells transfected with mock, N- or C-terminus PTEN chimeras or a bicistronic plasmid encoding PTEN or PTEN-C/S and GFP, were assayed for in vitro lipid phosphatase activity using PtdIns(3,4,5)P_3 as a substrate in a Malachite Green-based assay. The phosphate released (measured in pmoles) by the mock cell lysate was considered the reference unit. A western blot showing the corresponding cell extract PTEN levels is shown at the right. Data are representative of three separate experiments. (B) Extracts from unstimulated and CXCL12 (100 nM)-stimulated mock, PTEN-GFP- or PTEN-C/S-GFP-Jurkat cells were analyzed sequentially with anti-phosphoAKT and AKT Ab, and with anti-PTEN as a protein expression control. After densitometry, AKT phosphorylation was determined as the phospho-AKT:AKT ratio (×10) (n=3). (C) The AKT phosphorylation index was also determined using extracts from unstimulated and CXCL12-stimulated mock, GFP-PTEN or PTEN-GFP-Jurkat cells as above (n=2).

chimeric proteins by tagging GFP to the PTEN N- or C-terminus and characterized the in vitro activity of these chimeras expressed in Jurkat cells in a Malachite-Green-based phosphatase assay using PtdIns(3,4,5)P_3 as a substrate. We found that both PTEN-GFP (N-terminal tag) and GFP-PTEN (C-terminal tag) effectively dephosphorylated this substrate, whereas the catalytically inactive PTEN-C/S-GFP showed only minimal phosphatase activity compared with mock Jurkat cells (Fig. 1A). Notably, active GFP chimeras showed lipid phosphatase activity similar to that of untagged PTEN overexpressed at comparable levels (Fig. 1A).

To study the phosphatase activity of the chimeras in living cells, we took advantage of the fact that protein kinase B (PKB/AKT) phosphorylation and activation require PI3K products (Xu et al., 2002). Expression of PTEN-GFP, but not of a catalytically inactive mutant (PTEN-C/S-GFP), reduced basal phospho-AKT levels in Jurkat cells (Fig. 1B). As in other reports (Xu et al., 2002), PTEN-GFP did not eliminate AKT activation after CXCL12 stimulation (Fig. 1B), although it reduced the peak of CXCL12-induced AKT phosphorylation. In contrast to the PTEN-GFP chimera, basal phospho-AKT levels in Jurkat cells were not affected by GFP-PTEN chimera overexpression (Fig. 1C), although this chimera dephosphorylated PtdIns(3,4,5)P_3 in the in vitro lipid phosphatase assay (Fig. 1A).

Western blot analysis of Jurkat cells expressing PTEN chimeras with anti-PTEN and anti-GFP antibodies always developed a single band corresponding to the predicted molecular weight for the fusion between PTEN and GFP. This suggests that the chimeras were expressed as fusion proteins. To confirm this point, we performed immunofluorescence staining of unstimulated and chemoattractant-stimulated HL60 cells expressing these chimeras, using an anti-PTEN antibody. We found coincident cytoplasmic staining of PTEN-GFP (green label) and of an anti-PTEN antibody (red label) in both unstimulated and *f*MLP-stimulated cells (see supplementary material, Fig. S1). Similar results were obtained with the GFP-PTEN chimera (not shown).

GFP-PTEN and PTEN-GFP do not polarize during chemotaxis

We initially analyzed PTEN dynamics in chemotaxing human cells by expressing a C-terminal GFP-tagged PTEN fusion protein, similar to that used in the *Dictyostelium* studies. HL60 cells co-expressing PTEN-GFP and the inert cytosolic RFP probe were exposed to an *f*MLP gradient delivered by micropipette. PTEN-GFP levels were approximately 1.5-fold higher than those of endogenous PTEN (see supplementary material, Fig. S2A). Most PTEN-GFP was found in cytoplasm, with no redistribution during chemotaxis (Fig. 2A; see also supplementary material, Movie 1); some nuclear staining was also seen in several cells. In some frames, PTEN-GFP accumulated in the cytosol area facing the attractant source; in other frames, weaker cytosolic labeling was seen at the rear. Fluorescence intensity scanning showed that PTEN-GFP accumulation coincided with increased RFP labeling in the same cell areas (Fig. 2B); PTEN-GFP accumulation at the sides was not observed (Fig. 2C). PTEN-GFP levels in Jurkat cells were comparable to those detected for endogenous PTEN in HL60 cells (see supplementary material, Fig. S2B). PTEN-GFP did not accumulate in migrating Jurkat cells (see supplementary material, Fig. S3).

As lipid rafts polarize to the leading edge and the uropod of moving leukocytes (Gómez-Moutón et al., 2001; Mañes et al., 2003; van Buul et al., 2003), we co-expressed PTEN-GFP with

the raft marker RFP-GPI (glycosylphosphatidylinositol). Whereas the bulk of PTEN-GFP was distributed homogeneously, RFP-GPI polarized to the front and rear of moving, PTEN-GFP-expressing HL60 cells (Fig. 2D,E). These results indicate that specific markers are polarized in PTEN-GFP-expressing cells.

The PTEN C-terminal region has multiple phosphorylation sites for casein kinase II and a PDZ-binding domain that can interact with membrane-associated guanylate kinase inverted (MAGI) proteins (Georgescu et al., 1999; Torres and Pulido, 2001; Wu et al., 2000). As these interactions could be impeded in the PTEN-GFP chimera, we studied GFP-PTEN dynamics in *f*MLP-stimulated HL60 cells. GFP-PTEN levels were approximately twofold those of endogenous PTEN (see supplementary material, Fig. S2A). During *f*MLP-induced chemotaxis of HL60 cells co-expressing GFP-PTEN and RFP, most GFP-PTEN was evenly distributed in cytosol (Fig. 3A,B; see also supplementary material, Movie 3).

Cell location of PTEN is independent of its catalytic activity

We studied the dynamics of the inactive PTEN-C/S-GFP during chemotaxis of HL60 cells co-expressing the RFP-GPI raft marker. PTEN-C/S-GFP levels were approximately twofold those of endogenous PTEN (see supplementary material, Fig. S2A). RFP-GPI polarized during cell movement, whereas PTEN-C/S-GFP was evenly distributed in cytosol (Fig. 4A,B; see also supplementary material, Movie 4). Cytosolic PTEN-C/S-GFP distribution was similar to that of RFP in moving Jurkat cells (see supplementary material, Fig. S4). Taken together, the results suggest that PTEN-C/S-GFP localization remains homogeneous in chemotaxing cells.

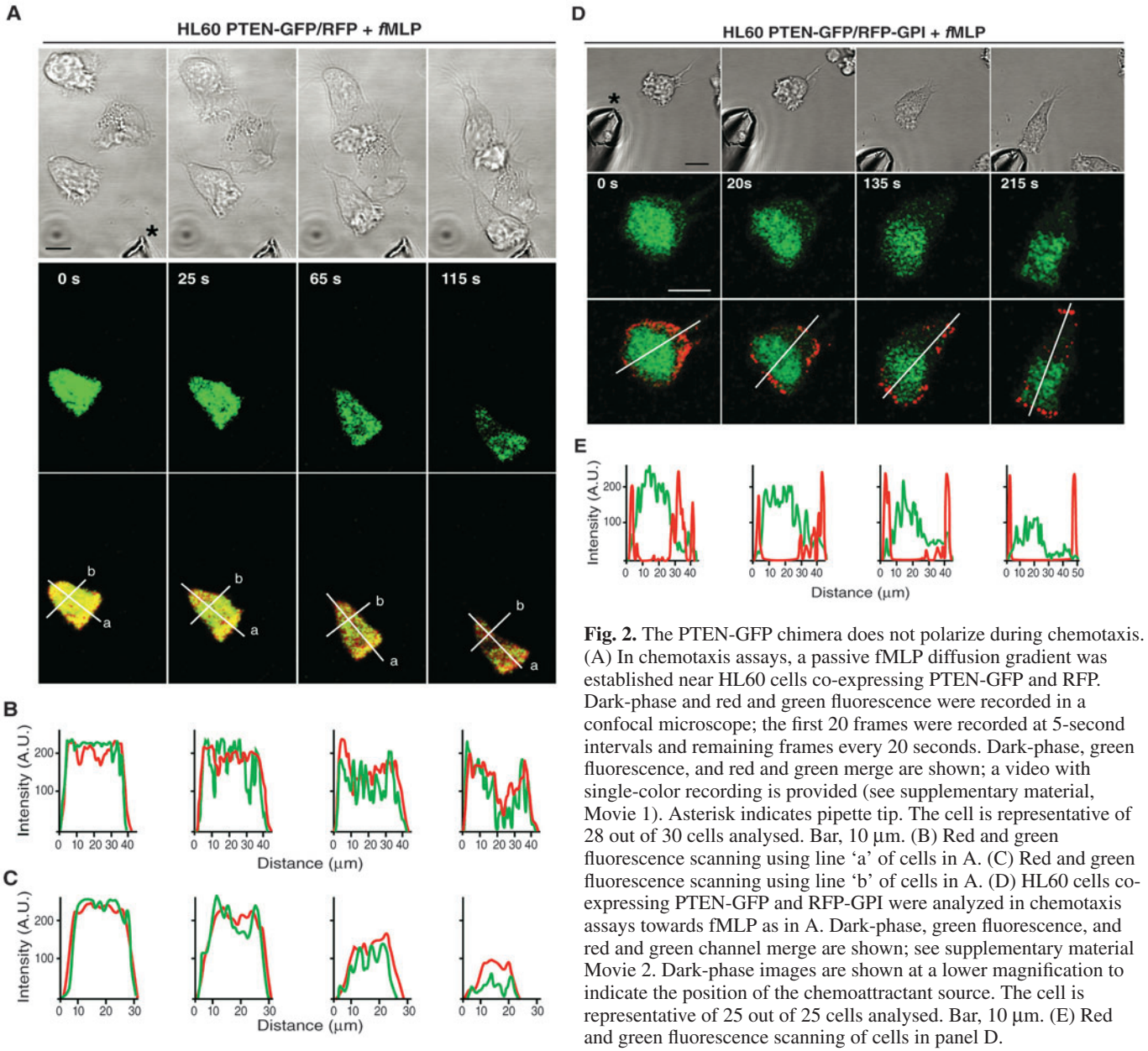

Fig. 2. The PTEN-GFP chimera does not polarize during chemotaxis. (A) In chemotaxis assays, a passive fMLP diffusion gradient was established near HL60 cells co-expressing PTEN-GFP and RFP. Dark-phase and red and green fluorescence were recorded in a confocal microscope; the first 20 frames were recorded at 5-second intervals and remaining frames every 20 seconds. Dark-phase, green fluorescence, and red and green merge are shown; a video with single-color recording is provided (see supplementary material, Movie 1). Asterisk indicates pipette tip. The cell is representative of 28 out of 30 cells analysed. Bar, 10 μm. (B) Red and green fluorescence scanning using line 'a' of cells in A. (C) Red and green fluorescence scanning using line 'b' of cells in A. (D) HL60 cells co-expressing PTEN-GFP and RFP-GPI were analyzed in chemotaxis assays towards fMLP as in A. Dark-phase, green fluorescence, and red and green channel merge are shown; see supplementary material Movie 2. Dark-phase images are shown at a lower magnification to indicate the position of the chemoattractant source. The cell is representative of 25 out of 25 cells analysed. Bar, 10 μm. (E) Red and green fluorescence scanning of cells in panel D.

PTEN chimeras and endogenous PTEN remain evenly distributed in cytoplasm after stimulation

To analyze the amount of PTEN chimera bound to the membrane before and after stimulation, we subfractionated PTEN-GFP- or PTEN-C/S-GFP-expressing Jurkat cells and found that most of these chimeras were confined to the cytosol of unstimulated or CXCL12-stimulated cells (Fig. 5). In contrast to PTEN chimeras, CXCL12 stimulation induced recruitment of the class IA PI3K p85 regulatory subunit to the membrane shortly after stimulation (Fig. 5). CXCL12 stimulation induced p85 membrane recruitment even in mock cells (Fig. 5), which have a high basal PI3K activity level, as these cells do not express PTEN. The results concur with those in Fig. 1B, showing that CXCL12 induced AKT phosphorylation even in PTEN null cells.

We also studied the location of endogenous PTEN in chemoattractant-stimulated HL60 cells, and found homogeneous distribution of endogenous PTEN in *f*MLP-stimulated PTEN-expressing HL60 cells stained with an anti-PTEN antibody (Fig. 6A). The specificity of this antibody was tested in CEM cells (Fig. 6B), a leukemia lymphoblastic cell line with homozygous deletion of the PTEN gene (Sakai et al., 1998). Cell fractionation showed that endogenous PTEN was confined largely to cytosol in unstimulated or *f*MLP-stimulated cells (Fig. 6C), whereas the p85 regulatory subunit translocated to the plasma membrane shortly after *f*MLP stimulation.

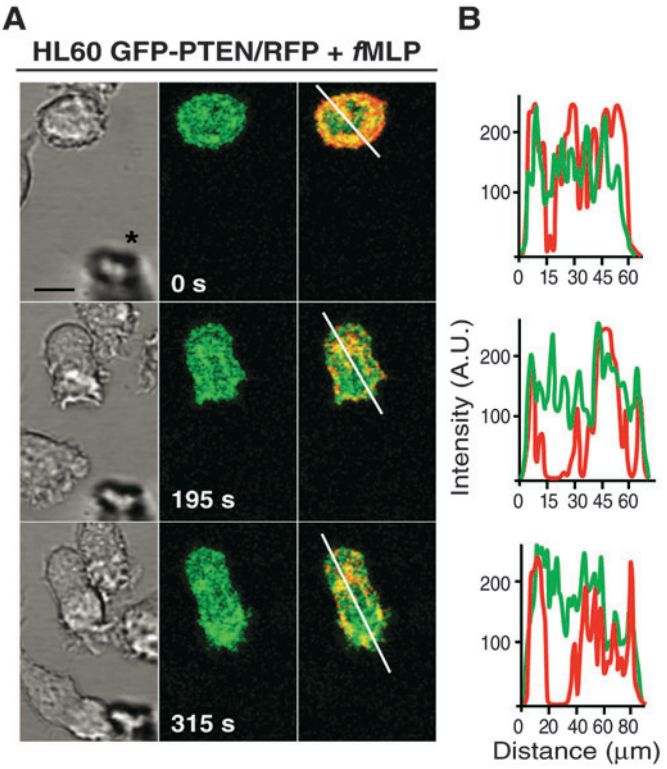

Fig. 3. GFP-PTEN remains evenly distributed during chemotaxis. (A) HL60 cells co-expressing GFP-PTEN and RFP were analyzed in chemotaxis assays towards fMLP. Dark-phase, green fluorescence, and red and green channel merge are shown; see supplementary material, Movie 3. The asterisk indicates the pipette tip. The cell is representative of 14 out of 15 cells analysed. Bar, 10 μm. (B) Red and green fluorescence scanning of cells in panel A.

PTEN regulates actin polymerization but not cell orientation

We induced PTEN depletion with specific siRNA in HL60 cells. PTEN siRNA-transfected HL60 cells showed a 50% reduction in PTEN protein levels compared with non-specific siRNA-transfected or untransfected cells (Fig. 7A). Despite this reduction, chemotaxis toward *f*MLP was comparable between cells with normal or reduced PTEN levels (Fig. 7B). As we could not abrogate PTEN expression completely in HL60 cells, we performed the opposite experiment, re-expressing PTEN in a true PTEN-null cell line. We compared chemotaxis between GFP-expressing Jurkat cells and cells transfected with a bicistronic plasmid (not a chimeric protein) containing PTEN or PTEN-C/S and GFP (Fig. 7C); again, chemotaxis was independent of PTEN protein levels or PTEN activity (Fig. 7D). Nonetheless, Jurkat chemotaxis was sensitive to the PI3K inhibitor LY294002 (see supplementary material, Fig. S5), confirming previous observations (Sotsios et al., 1999). LY294002 treatment also inhibited basal migration in the absence of stimulus, suggesting that this drug could affect the general motility of Jurkat cells.

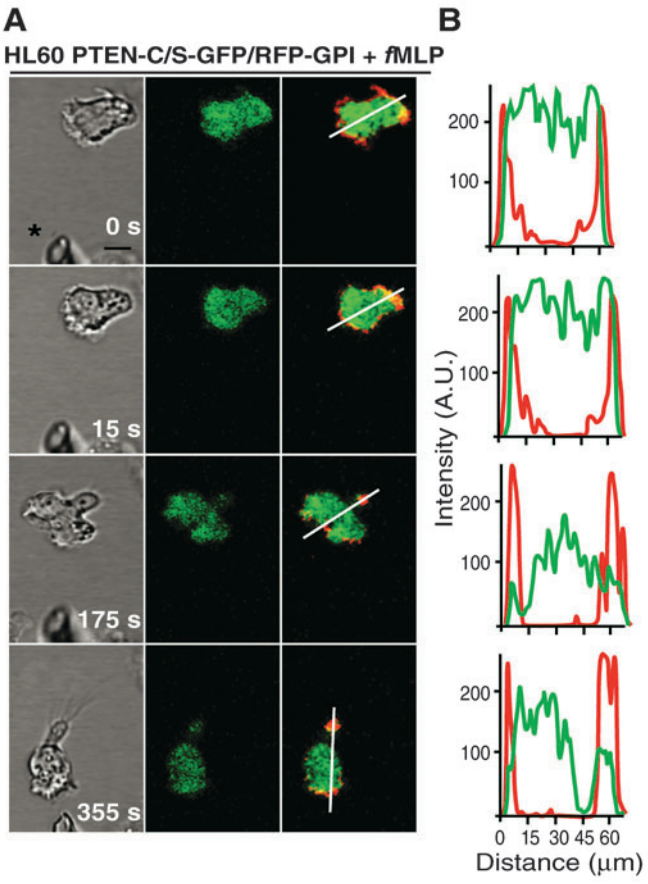

Fig. 4. PTEN-C/S-GFP does not polarize during chemotaxis. (A) HL60 cells co-expressing PTEN-C/S-GFP and RFP-GPI were analyzed in chemotaxis assays towards fMLP as in Fig. 2A. Dark-phase, green fluorescence, and red and green channel merge are shown; see supplementary material, Movie 4. The asterisk indicates the pipette tip. The cell is representative of 20 out of 22 cells analysed. Bar, 10 μm. (B) Red and green fluorescence scanning of cells in panel A.

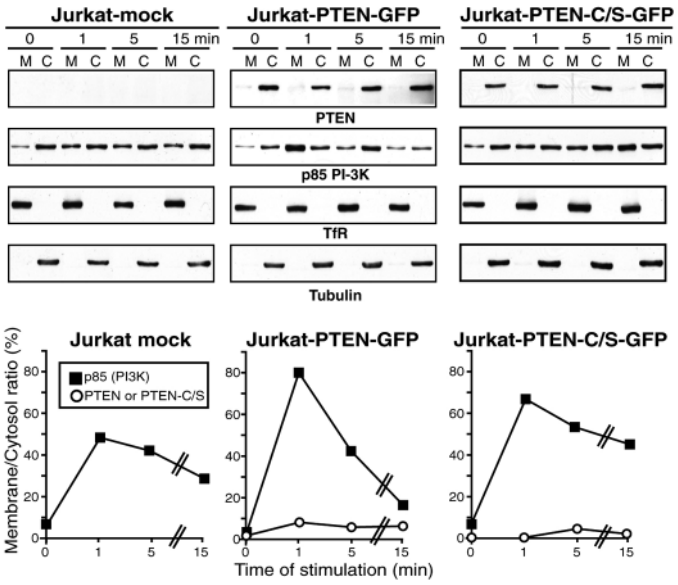

Fig. 5. PTEN chimeras are found mostly in the cytosol of Jurkat cells. Unstimulated or CXCL12 (100 nM)-stimulated mock-, PTEN-GFP- and PTEN-C/S-GFP-expressing Jurkat cells were fractionated in density gradients to isolate membrane (M) and cytosolic (C) fractions, and western blots were performed with anti-PTEN, -p85 PI3K, -transferrin receptor (TfR) and -tubulin antibodies (n=3). Relative accumulation of p85 and PTEN-GFP in the membrane and cytosolic fractions during a CXCL12 stimulation time course was calculated by densitometry.

Single cell assays showed that orientation and persistence of movement toward the chemotactic source was PTEN-independent (Fig. 7E), although PTEN-expressing cells moved more slowly than PTEN-null cells (Fig. 7E). PTEN expression influenced CXCL12-induced actin polymerization. CXCL12 stimulation of Jurkat cells induced a rapid increase in actin polymerization that peaked in seconds, followed by a slow phase in which polymerization was sustained for minutes (Fig. 7F). Expression of active PTEN, but not the catalytically inactive mutant, attenuated both actin polymerization phases, and F-actin returned to basal levels more rapidly in PTEN-expressing Jurkat cells than in controls (Fig. 7F). Collectively, the results suggest that PTEN has no major role in cell orientation but participates in actin cytoskeleton remodeling and cell speed.

Discussion

PI3K and PTEN are proposed as components of an excitation-inhibition system, to explain how a cell senses and responds to shallow chemoattractant gradients. In this model, PTEN is a global inhibitor that concentrates at the sides and rear of cells to confine PI3K activation to the front of cells (Funamoto et al., 2002; Iijima and Devreotes, 2002). Whereas PTEN shows this pattern in *Dictyostelium*, two apparently contradictory results were reported in mammalian cells (Li et al., 2003; Xu et al., 2003). We performed a systematic analysis of real-time distribution of N- and C-terminus-tagged PTEN chimeras, with or without catalytic activity, in chemotaxing PTEN-expressing or PTEN-null cells. We found

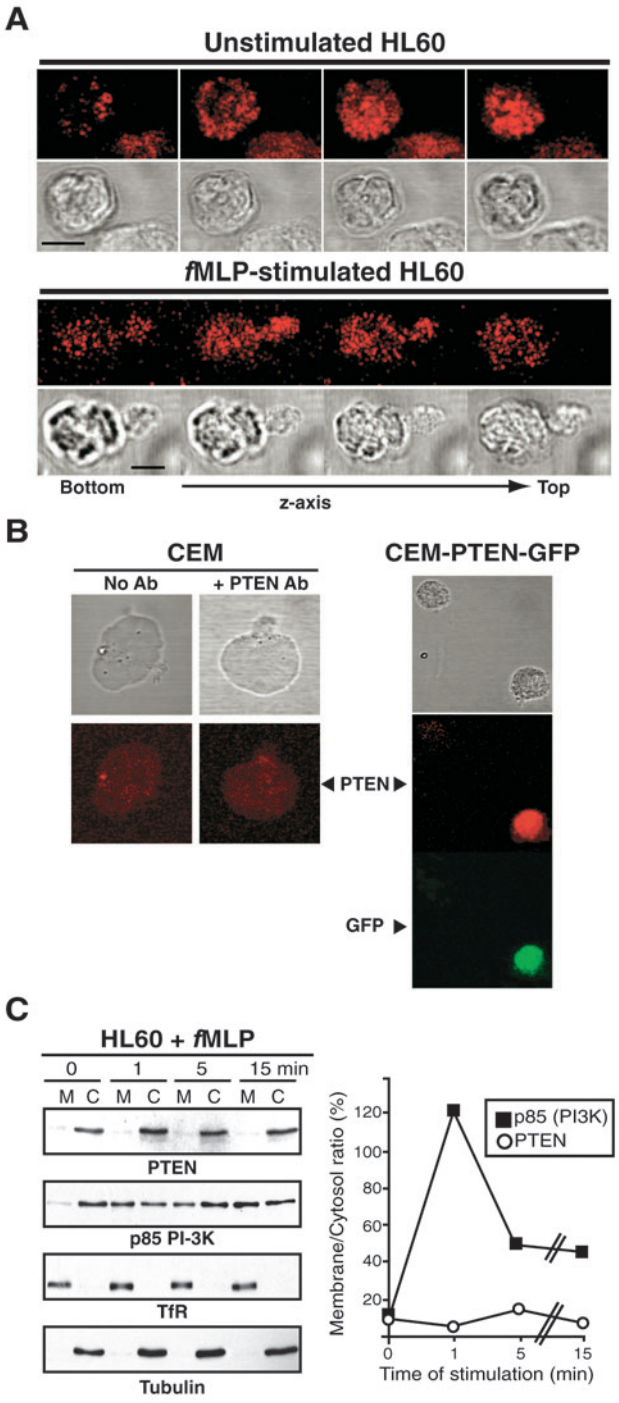

Fig. 6. Endogenous PTEN is distributed homogeneously in the cytosol of HL60 cells. (A) Immunofluorescence analysis with anti-PTEN antibody (red) to show the endogenous PTEN location in unstimulated or fMLP-stimulated HL60 cells. The cells are representative of 25 out of 25 cells analysed. Bar, 10 μm. (B) Immunofluorescence of mock- and PTEN-GFP-transfected CEM cells was performed to demonstrate anti-PTEN antibody (red staining) specificity. Bar, 10 μm. (C) Analysis of PTEN and p85 in the membrane and cytosolic fractions of fMLP-stimulated HL60 cells was performed as described in Fig. 5.

no evidence of endogenous or chimeric PTEN accumulation or localization in directionally- or homogenously-stimulated

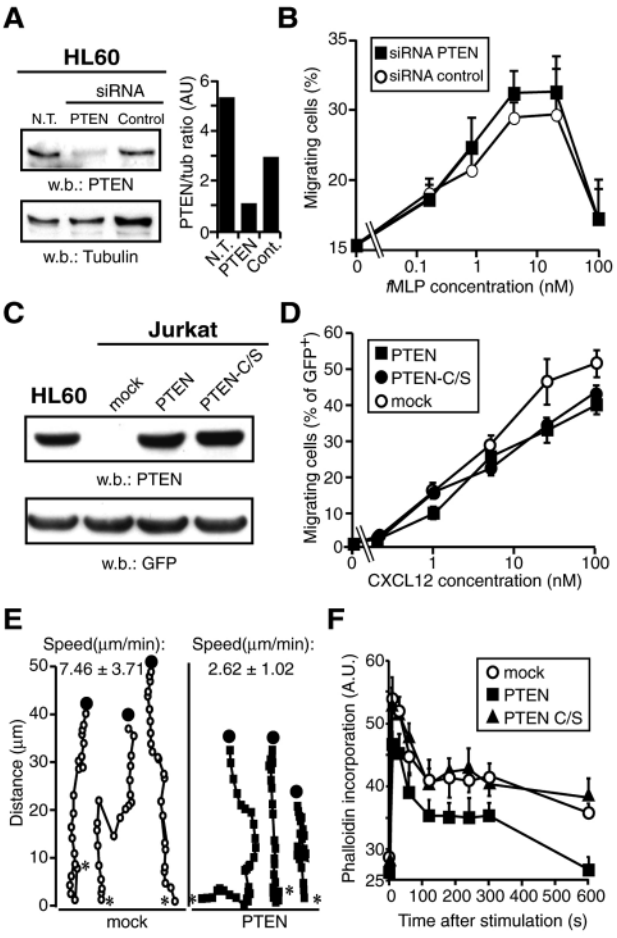

Fig. 7. PTEN regulates actin polymerization but not cell orientation. (A) HL60 cells were untransfected (N.T.) or transfected with control or PTEN-specific siRNA. PTEN and tubulin (loading control) were analyzed by western blot. The graph at the right shows the quantification of PTEN estimated by densitometry using tubulin values for normalization. (B) The cells in panel A were analyzed for chemotaxis toward fMLP in transwells. Cells (2×10^5) were added to the upper chamber; the number of migrated cells in the lower well was determined by FACS and depicted as a percentage of migrating cells. (C) Jurkat cells were transfected with a bicistronic plasmid encoding PTEN or PTEN-C/S and GFP. PTEN and GFP expression were analyzed by western blot. Equal protein amounts of a GFP-transfected HL60 cell lysate were included in the western blot to compare relative amounts of endogenous (HL60) and ectopically expressed PTEN (Jurkat). (D) The cells (2×10^5) in panel C were analyzed for chemotaxis toward CXCL12 in transwell assays; GFP-positive cells in the lower well were determined by FACS; results are expressed as the percentage of migrating cells. (E) The cells in panel C were analyzed for chemotaxis toward CXCL12 as in Fig. 2A; dark-phase and green fluorescence were recorded at 23-second intervals. Migration parameters for ⩾20 cells/condition were determined with specific software. Representative paths of three cells are shown; average speed is shown of all cells analyzed. *, start point; ●, pipette tip. (F) CXCL12-induced actin polymerization was measured by FACS in mock, PTEN-, and PTEN-C/S-expressing cells described in panel C, using Alexa-fluor 633-phalloidin.

cells. PTEN was evenly distributed throughout the chemotaxing cell cytosol, with a pattern similar to that of the inert cytosolic RFP probe.

We found that both N- and C-terminus GFP-tagged chimeric PTEN are homogeneously dispersed in the cytosol of *f*MLP or CXCL12-stimulated cells. This contrasts with *Dictyostelium* cells, in which around 10% of PTEN associates the cell perimeter after chemoattractant stimulation (Iijima and Devreotes, 2002). Our data are nonetheless consistent with other studies in mammalian cells, which indicate that the bulk of PTEN is in the cytoplasm and/or nucleus (Deichmann et al., 2002; Gimm et al., 2000; Wu et al., 2000). The mechanisms regulating PTEN activity and subcellular distribution are not yet fully known. As its substrate is at the plasma membrane, a PTEN fraction should be found at this site; indeed, a GFP-tagged PTEN mutant bearing the phosphatase and C2 domains persists at the membrane (Das et al., 2003). The PTEN N-terminus contains a putative PtdIns(4,5)P_2 binding motif, important for PTEN membrane association in *Dictyostelium* (Iijima and Devreotes, 2002). Indeed, PTEN-GFP, but not GFP-PTEN, reduced phospho-AKT levels in Jurkat cells, which suggests a role for the PTEN N-terminal region in the regulation of phosphatase activity. C-terminal phosphorylation is suggested to regulate PTEN membrane binding, activation and stability, as it serves as an electrostatic switch for PTEN membrane interaction (Das et al., 2003; Torres and Pulido, 2001). Although the PTEN-GFP reduced basal phospho-AKT levels, an indirect readout of PtdIns(3,4,5)P_3 levels, we cannot rule out that the presence of GFP at the C-terminus could prevent specific phosphorylation/dephosphorylation events required for PTEN localization.

We therefore analyzed in detail the location of endogenous PTEN in HL60 cells. Immunofluorescence analysis showed that endogenous PTEN was largely confined to the cytosol of unstimulated or *f*MLP-stimulated HL60 cells, and this was again confirmed by cell fractionation. Moreover, we did not detect preferential accumulation of the endogenous protein at the cell rear or sides in polarized cells. This result is consistent with a previous report in which no PTEN accumulation was found in differentiated HL60 cells (Xu et al., 2003), in apparent contradiction of preferential PTEN accumulation at the uropod in primary neutrophils (Li et al., 2003). This raised the intriguing possibility that PTEN location in chemotaxing cells may be governed by cell type-specific factors. It should be noted, however, that we observed AKT PH domain recruitment to the leading edge of differentiated HL60 cells (Gómez-Moutón et al., 2004), indicating that PI3K signaling is restricted to the cell front in these cells.

Our inability to detect membrane-associated PTEN after cell subfractionation may be caused by rapid PTEN shuttling between the cytosol and the membrane. Dephosphorylation of the C-terminus is crucial for PTEN recruitment to the membrane but enhances its proteolytic turnover (Das et al., 2003; Torres and Pulido, 2001). This turnover would preclude the observation of PTEN accumulation at the membrane in cell fractionation or immunofluorescence analyses. Despite this turnover, one would predict certain PTEN accumulation in the cytosolic areas at which PTEN is actively recruited in chemotaxing cells. Moreover, if only a very small PTEN fraction is functionally active in moving cells, it is questionable whether this amount of PTEN is sufficient to function as a global PI3K inhibitor during migration, as proposed for

Dictyostelium. This is especially relevant, as chemoattractants induced robust recruitment of PI3K to the cell membrane (Fig. 5, Fig. 6C) and persistent accumulation of active PI3K at the leading edge of moving HL60 cells (Gómez-Moutón et al., 2004).

We therefore analyzed the effect of PTEN in HL60 and Jurkat cell migration. First, we tried to inhibit PTEN expression in HL60 cells using siRNA. Although PTEN expression was reduced around 50%, HL60 chemotaxis toward *f*MLP was unaffected. Since small amounts of PTEN were detected in these cells, it can be argued that this is sufficient to provide the small fraction of functional PTEN needed for chemotaxis. To rule out this possibility, we used Jurkat cells, a PTEN-deficient cell line. We found that PTEN re-expression reduced the speed of moving cells, as reported for other cell types (Liliental et al., 2000; Tamura et al., 1998); however, PTEN-expressing Jurkat cells sensed and responded to chemoattractant gradients as did mock-transfected Jurkat cells. These results contrast with those reported for *Dictyostelium*, in which PTEN expression increases the speed and controls the directionality of moving cells (Funamoto et al., 2002; Iijima and Devreotes, 2002).

Evidence suggests that the PI3K pathway might be important for the chemotaxis of specific cell types. In lymphocytes, contradictory results have been obtained using PI3K inhibitors (Sotsios et al., 1999; Cronshaw et al., 2004). Moreover, it was recently shown that lymphocyte homing is controlled mainly by DOCK-2 activity, whereas PI3Kγ activation has a minor role in this process (Nombela-Arrieta et al., 2004; Ward, 2004). In HL60 cells and neutrophils, it was proposed that PI3K is required for directionality (Li et al., 2003; Xu et al., 2003). Our results suggesting that PTEN has a minor influence on cell orientation do not contradict this view; indeed, we found that chemoattractant stimulation induced further PI3K activation in PTEN-null cells, despite the high basal PI3K activity in these cells. PTEN overexpression did not prevent chemoattractant-induced PI3K activation, as determined by AKT phosphorylation, although it reduced the basal PI3K activity of PTEN-null cells. These results concur with previous observations indicating that PTEN does not abolish PI3K activation following stimulation, but has a major role in regulating basal PtdIns(3,4,5)P_3 levels (Myers et al., 1998; Stambolic et al., 1998; Xu et al., 2002). This may explain the sustained actin polymerization phase observed in mock (*pten* null) and PTEN-C/S-expressing compared to PTEN-expressing Jurkat cells.

We propose that, at least in some mammalian cells, PTEN is not essential for a cell to sense and respond to shallow chemoattractant gradients. Accumulation of PI3K products at the leading edge of these moving cells may be a consequence of preferential activation of specific receptors at this cell site (Gómez-Moutón et al., 2004; van Buul et al., 2003). PTEN may nonetheless have other functions in mammalian cell chemotaxis by controlling actin cytoskeleton remodeling, either through its lipid or protein phosphatase activities (Raftopoulou et al., 2004).

We thank J. Stein for critical reading of the manuscript, R. Pulido for PTEN cDNA, J. Díez-Guerra and C. Sánchez for help with Metamorph, and C. Mark for editorial assistance. S.J.-B. is the recipient of a pre-doctoral fellowship from the FPU Program. This work was supported by grants from the Spanish Ministry of Education and Science, and the EU (QLG1CT 2001-02171). The Department of Immunology and Oncology was founded and is supported by the Spanish Council for Scientific Research (CSIC), the Spanish Ministry of Health, and Pfizer.

References

Anzelon, A., Wu, H. and Rickert, R. (2003). Pten inactivation alters peripheral B lymphocyte fate and reconstitutes CD19 function. *Nat. Immunol.* **4**, 287-294.

Borlado, L., Redondo, C., Alvarez, B., Jimenez, C., Criado, L., Flores, J., Marcos, M., Martinez-A., C., Balomenos, D. and Carrera, A. (2000). Increased phosphoinositide 3-kinase activity induces a lymphoproliferative disorder and contributes to tumor generation in vivo. *FASEB J.* **14**, 895-903.

Cronshaw, D. G., Owen, C., Brown, Z. and Ward, S. G. (2004). Activation of phosphoinositide 3-kinases by the CCR4 ligand macrophage-derived chemokine is a dispensable signal for T lymphocyte chemotaxis. *J. Immunol.* **172**, 7761-7770.

Das, S., Dixon, J. and Cho, W. (2003). Membrane-binding and activation mechanism of PTEN. *Proc. Natl. Acad. Sci. USA* **100**, 7491-7496.

Deichmann, M., Thome, M., Benner, A., Egner, U., Hartschuh, W. and Naher, H. (2002). PTEN/MMAC1 expression in melanoma resection specimens. *Br. J. Cancer* **87**, 1431-1436.

Fox, J., Ung, K., Tanlimco, S. and Jirik, F. (2002). Disruption of a single Pten allele augments the chemotactic response of B lymphocytes to stromal cell-derived factor-1. *J. Immunol.* **169**, 49-54.

Friedl, P., Brocker, E. and Zanker, K. (1998). Integrins, cell matrix interactions and cell migration strategies: fundamental differences in leukocytes and tumor cells. *Cell Adhes. Commun.* **6**, 225-236.

Funamoto, S., Meili, R., Lee, S., Parry, L. and Firtel, R. (2002). Spatial and temporal regulation of 3-phosphoinositides by PI3-Kinase and PTEN mediates chemotaxis. *Cell* **109**, 611-623.

Georgescu, M., Kirsch, K., Akagi, T., Shishido, T. and Hanafusa, H. (1999). The tumor-suppressor activity of PTEN is regulated by its carboxyl-terminal region. *Proc. Natl. Acad. Sci. USA* **96**, 10182-10187.

Gimm, O., Perren, A., Weng, L., Marsh, D., Yeh, J., Ziebold, U., Gil, E., Hinze, R., Delbridge, L., Lees, J. et al. (2000). Differential nuclear and cytoplasmic expression of PTEN in normal thyroid tissue, and benign and malignant epithelial thyroid tumours. *Am. J. Pathol.* **156**, 1693-1700.

Gómez-Moutón, C., Abad, J., Mira, E., Lacalle, R., Gallardo, E., Jiménez-Baranda, S., Illa, I., Bernad, A., Mañes, S. and Martínez-A., C. (2001). Segregation of leading-edge and uropod components into specific lipid rafts during T cell polarization. *Proc. Natl. Acad. Sci. USA* **98**, 9642-9647.

Gómez-Moutón, C., Lacalle, R., Mira, E., Jiménez-Baranda, S., Barber, D., Carrera, A., Martínez-A., C. and Mañes, S. (2004). Dynamic redistribution of raft domains as an organizing platform for signaling during cell chemotaxis. *J. Cell Biol.* **164**, 759-768.

Gu, J., Tamura, M., Pankov, R., Danen, E., Takino, T., Matsumoto, K. and Yamada, K. (1999). Shc and FAK differentially regulate cell motility and directionality modulated by PTEN. *J. Cell Biol.* **146**, 389-403.

Iijima, M. and Devreotes, P. (2002). Tumor suppressor PTEN mediates sensing of chemoattractant gradients. *Cell* **109**, 599-610.

Li, Z., Hannigan, M., Mo, Z., Liu, B., Lu, W., Wu, Y., Smrcka, A., Wu, G., Li, L., Liu, M. et al. (2003). Directional sensing requires Gβγ-mediated PAK1 and PIXα-dependent activation of Cdc42. *Cell* **114**, 215-227.

Liliental, J., Moon, S., Lesche, R., Mamillapalli, R., Li, D., Zheng, Y., Sun, H. and Wu, H. (2000). Genetic deletion of the Pten tumor suppressor gene promotes cell motility by activation of Rac1 and Cdc42 GTPases. *Curr. Biol.* **10**, 401-404.

Maehama, T. and Dixon, J. (1998). The tumor suppressor, PTEN/MMAC1, dephosphorylates the lipid second messenger, phosphatidylinositol 3,4,5-trisphosphate. *J. Biol. Chem.* **273**, 13375-13378.

Mañes, S., Lacalle, R., Gómez-Moutón, C. and Martínez-A., C. (2003). From rafts to crafts: membrane asymmetry in moving cells. *Trends Immunol.* **24**, 320-326.

Mira, E., Lacalle, R., González, M., Gómez-Moutón, C., Abad, J., Bernad, A., Martínez-A., C. and Mañes, S. (2001). A role for chemokine receptor transactivation in growth factor signaling. *EMBO Rep.* **2**, 151-156.

Myers, M., Pass, I., Batty, I., van der Kaay, J., Stolarov, J., Hemmings, B., Wigler, M., Downes, C. and Tonks, N. (1998). The lipid phosphatase activity of PTEN is critical for its tumor supressor function. *Proc. Natl. Acad. Sci. USA* **95**, 13513-13518.

Nombela-Arrieta, C., Lacalle, R. A., Montoya, M. C., Kunisaki, Y., Megías, D., Marqués, M., Carrera, A. C., Mañes, S., Fukui, Y., Martínez-A., C. et al. (2004). Differential requirements for DOCK2 and phosphoinositide-3-kinaseγ during T and B lymphocyte homing. *Immunity* **21**, 429-441.

Raftopoulou, M., Etienne-Manneville, S., Self, A., Nicholls, S. and Hall, A. (2004). Regulation of cell migration by the C2 domain of the tumor suppressor PTEN. *Science* **303**, 1179-1181.

Sakai, A., Thieblemont, C., Wellmann, A., Jaffe, E. and Raffeld, M. (1998). PTEN gene alterations in lymphoid neoplasms. *Blood* **92**, 3410-3415.

Seminario, M. and Wange, R. (2002). Signaling pathways of D3-phosphoinositide-binding kinases in T cells and their regulation by PTEN. *Semin. Immunol.* **14**, 27-36.

Sotsios, Y., Whittaker, G., Westwick, J. and Ward, S. (1999). The CXC chemokine stromal cell-derived factor activates a Gi-coupled phosphoinositide 3-Kinase in T lymphocytes. *J. Immunol.* **163**, 5954-5963.

Stambolic, V., Suzuki, A., de la Pompa, J., Brothers, G., Mirtsos, C., Sasaki, T., Ruland, J., Penninger, J., Siderovski, D. and Mak, T. (1998). Negative regulation of PKB/Akt-dependent cell survival by the tumor suppressor PTEN. *Cell* **95**, 29-39.

Suzuki, A., Kaisho, T., Ohishi, M., Tsukio-Yamaguchi, M., Tsubata, T., Koni, P., Sasaki, T., Mak, T. and Nakano, T. (2003). Critical roles of Pten in B cell homeostasis and immunoglobulin class switch recombination. *J. Exp. Med.* **197**, 657-667.

Tamura, M., Gu, J., Matsumoto, K., Aota, S., Parsons, R. and Yamada, K. (1998). Inhibition of cell migration, spreading, and focal adhesions by tumor suppressor PTEN. *Science* **280**, 1614.

Tamura, M., Gu, J., Takino, T. and Yamada, K. (1999). Tumor suppressor PTEN inhibition of cell invasion, migration, and growth: differential involvement of focal adhesion kinase and p130Cas. *Cancer Res.* **59**, 442-449.

Torres, J. and Pulido, R. (2001). The tumor suppressor PTEN is phosphorylated by the protein kinase CK2 at its C terminus. Implications for PTEN stability to proteasome-mediated degradation. *J. Biol. Chem.* **276**, 993-998.

van Buul, J., Voermans, C., van Gelderen, J., Anthony, E., van der Schoot, C. and Hordijk, P. (2003). Leukocyte-endothelium interaction promotes SDF-1-dependent polarization of CXCR4. *J. Biol. Chem.* **278**, 30302-30310.

Ward, S. G. (2004). Do phosphoinositide 3-kinases direct lymphocyte navigation? *Trends Immunol.* **25**, 67-74.

Wu, X., Hepner, K., Castelino-Prabhu, S., Do, D., Kaye, M., Yuan, X., Wood, J., Ross, C., Sawyers, C. and Whang, Y. (2000). Evidence for regulation of the PTEN tumor suppressor by a membrane-localized multi-PDZ domain containing scaffold protein MAGI-2. *Proc. Natl. Acad. Sci. USA* **97**, 4233-4238.

Xu, J., Wang, F., van Keymeulen, A., Herzmark, P., Straight, A., Kelly, K., Takuwa, Y., Sugimoto, N., Mitchison, T. and Bourne, H. (2003). Divergent signals and cytoskeletal assemblies regulate self-organizing polarity in neutrophils. *Cell* **114**, 201-214.

Xu, Z., Stokoe, D., Kane, L. and Weiss, A. (2002). The inducible expression of the tumor suppressor gene PTEN promotes apoptosis and decreases cell size by inhibiting the PI3K/Akt pathway in Jurkat T cells. *Cell Growth Differ.* **13**, 285-296.